Anal Bioanal Chem (2017) 409:5007–5018
DOI 10.1007/s00216-017-0444-1

RESEARCH PAPER

Unveiling the compositional variety of cardiolipins in *Rhodobacter sphaeroides* by liquid chromatography with electrospray ionization and multistage collision-induced dissociation mass spectrometry

Sara Granafei[1] · Ilario Losito[1,2] · Massimo Trotta[3] · Angela Agostiano[1,3] · Francesco Palmisano[1,2] · Tommaso R. I. Cataldi[1,2]

Received: 9 March 2017 / Revised: 16 May 2017 / Accepted: 1 June 2017 / Published online: 20 June 2017

Abstract Cardiolipins (CL) contained in the lipid extracts of the photosynthetic bacterium *Rhodobacter sphaeroides* (strain R26) were systematically characterized by reversed-phase liquid chromatography coupled to electrospray ionization mass spectrometry, performed in single (MS), tandem (MS/MS) and sequential (MS^3) modes using a linear ion trap mass spectrometer. The total number of carbon atoms and C=C bonds of each CL and, subsequently, those related to each of the constituting phosphatidic acid (PA) units, along with the location of the latter on the central glycerol backbone, were inferred from MS and MS/MS data, respectively. Moreover, the composition and location of both acyl chains on the glycerol backbone of each PA unit was obtained by MS^3 measurements, an approach used for the first time for the structural elucidation of CL in *R. sphaeroides*. As a result, an unprecedented profile of CL in this bacterium was obtained, with 27 main species characterized, many of which are represented by compositional or regiochemical isomers. Interestingly, such a variability is generated from a limited number of different acyl chains, either saturated (i.e. 12:0, 16:0, 17:0, 18:0, 19:0) or mono-unsaturated (16:1, 18:1). The absence of polyunsaturated chains, more susceptible to oxidation damage, appeared to be indirectly related to the lack of carotenoids potentially acting as antioxidant agents, a specific feature of *R. sphaeroides* R26. The occurrence of odd-numbered acyl chains was ascribed to the need to guarantee membrane fluidity, through a less compact packing of CL, thus compensating for the lack of CL bearing polyunsaturated side chains.

Keywords Cardiolipins · *Rhodobacter sphaeroides* · Bacterial extract · RP liquid chromatography · Tandem MS

Introduction

Cardiolipins (CL), or 1,3-bis(*sn*-3′-phosphatidyl)-*sn*-glycerols, are complex lipids whose molecular structure comprises two phosphatidic acid (PA) moieties covalently linked to a central glycerol backbone (see inset of Fig. 1) [1, 2]. CL are the only phospholipids found in the inner membrane of mitochondria, where they play a fundamental role in guaranteeing the correct functioning of several enzymes involved in energy metabolism [3]. Not surprisingly, altered biosynthesis, remodelling and degradation of CL acyl chains are involved in the Barth syndrome [4–6], whereas a decrease of mitochondrial CL content, most likely as a consequence of lipid peroxidation by oxidative stress, is believed to be a contributing factor in the development of Parkinson's disease [7]. The possible role played by CL in these and in other relevant pathologies has stimulated the interest for their analytical characterization, usually achieved using liquid chromatography coupled to electrospray ionization (ESI) mass spectrometry (MS) [4, 8, 9], also performed under high-resolution conditions [10]. Applications of LC-ESI-MS to the identification of CL in mammalian cells [11] and in murine tumour cell lines [12] as well as to the characterization of oxidation products of standard CL [13] have been reported.

Electronic supplementary material The online version of this article (doi:10.1007/s00216-017-0444-1) contains supplementary material, which is available to authorized users.

✉ Tommaso R. I. Cataldi
tommaso.cataldi@uniba.it

[1] Dipartimento di Chimica, Università degli Studi di Bari Aldo Moro, Via E. Orabona 4, 70126 Bari, Italy

[2] Centro Interdipartimentale SMART, Università degli Studi di Bari Aldo Moro, Via E. Orabona 4, 70126 Bari, Italy

[3] Istituto Processi Chimico Fisici CNR, Università degli Studi di Bari Aldo Moro, Via E. Orabona 4, 70126 Bari, Italy

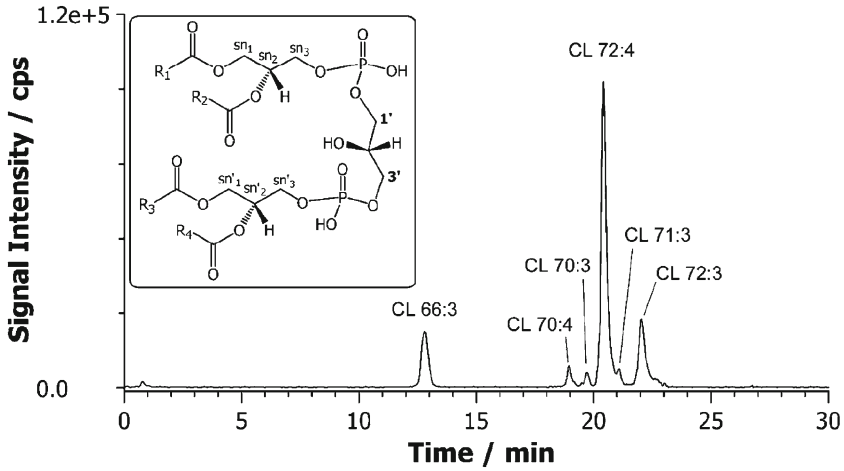

Fig. 1 Multiple extracted ion current chromatogram (multi-XIC) resulting from the RPLC-ESI(−)MS analysis of cardiolipins (*CL*) extracted from *R. sphaeroides* R26. The chromatogram was obtained by summing the currents related to the $[M-H]^-$ ions of the six major CL species, each extracted by using a 1 *m/z* unit wide window centred on the selected *m/z* value. See Table 1 for a complete list of the CL identified in the bacterial lipid extract. The *inset* shows the general structure of cardiolipins

The above cited LC-MS approaches have generally proved very helpful in facing the analytical challenge posed by the structural variability of cardiolipins, related to the presence of four different acyl chains, each characterized by specific chain length and number, position and geometry of double bonds. It is worth noting that CL are typical components of bacterial membranes, where they contribute to maintain the electrochemical potential used for substrate transport and ATP synthesis [11, 14]. CL are also present in photosynthetic bacteria, where the core of the energy conversion apparatus is represented by a multi-subunit transmembrane enzyme known as the *reaction centre* (RC). Interaction between CL and RC has interesting consequences, including an improved thermal stability of the enzyme. CL interact also with the respiratory protein *cytochrome c* oxidase (*CcO*) of such bacteria grown under non-photosynthetic conditions; indeed, *CcO* is inactivated upon CL removal [15, 16]. Likewise, the correlation between the increase of CL levels and the exposure of prokaryotes (both bacteria and archaea) to osmotic stress has been proposed [14, 16].

Among photosynthetic bacteria, *Rhodobacter sphaeroides*, a gram-negative, phototropic purple non-sulphur bacterium belonging to the α-3 subgroup of Proteobacteria [17], has attracted great attention in the last years as a model organism for photosynthesis and metabolic capability studies. Being able to grow under either aerobic or anaerobic respiration, fermentation or photosynthesis conditions, *R. sphaeroides* is highly versatile [17–23]. In particular, its R26 strain is a stable deletion mutant, lacking photoprotective carotenoid pigments [24] that play two important functions: (i) contributing to the harvest of light between 400 and 500 nm and (ii) protecting the entire assembly against photo-oxidation by quenching singlet oxygen molecules ($^1O_2$) when the bacterium is exposed to light and oxygen. The absence of carotenoids in *R. sphaeroides* R26 makes this mutant very sensitive to oxidative damage, thus imposing a strict anaerobic photosynthetic growth [25–27], during which invaginations of the intracytoplasmic membrane (ICM), hosting the entire photosynthetic apparatus, occur [14]. The ICM is also rich in CL, representing 2 to 14% of the total lipid extracts of cells and chromatophores of *R. sphaeroides* [16]. In fact, the only CL recognized in *R. sphaeroides* so far are CL $(18:1)_4$, CL $(16:1)_1(18:1)_3$, CL$(16:0)_1(18:1)_3$ and CL $(18:0)_1(18:1)_3$, whose analysis has been based either on thin-layer chromatographic separation followed by ESI-MS/MS [14, 16] or on matrix-assisted laser desorption ionization (MALDI)-MS/MS [28, 29]. Following the general format suggested by Liebisch et al. [30], the notation used for the above cited CL indicates that only the compositions (C:D) of the different chains in terms of numbers of carbon atoms (C) and of C=C double bonds (D) could be inferred, whereas their specific location on the sn_1/sn_2 positions of the two lateral glycerol moieties of the general CL structure (see Fig. 1 inset) remains undefined.

Since the role played by CL in *R. sphaeroides* depends on the length and number of double bonds of their acyl chains, a deeper characterization of these phospholipids, aiming at discovering additional side chain compositions, has been undertaken in our laboratory. The TLC fraction containing CL of the bacterial extracts was separated by using reversed-phase liquid chromatography (RPLC) on a solid-core stationary phase (2.6 μm particle size), and then characterized by multistage ESI-MS analysis of singly negatively charged molecules, performed using a linear ion trap [31]. For the first time, MS^3 has been adopted in the structural characterization of CL in the bacterial extracts of *R. sphaeroides*. As a result, several CL species, often showing subtle structural differences and potentially having large implications for biological functions [32], have been identified in the *R. sphaeroides* R26 mutant. Details of their characterization will be provided in the present paper.

Materials and methods

Chemicals

Water and methanol, both LC-MS grade, chloroform (HPLC grade) and ammonium acetate (reagent grade) were obtained from Sigma-Aldrich (Milan, Italy).

LC-MS instrumentation and operating conditions

All experiments were performed using an Ultimate 3000 UHPLC system coupled to a Velos Pro double stage linear ion trap (LIT) mass spectrometer (Thermo Scientific, Waltham, MA, USA). An Accucore RP-MS column (100 × 2.1 mm ID, 2.6 μm particle size) equipped with an Accucore RP-MS (10 × 2.1 mm ID) security guard cartridge (Thermo Scientific, Waltham, MA, USA) and thermostated at 30 °C was selected for performing LC separations of bacterial lipid extracts, manually injected via a 5-μL sample loop. The following binary gradient elution program, based on water (solvent A) and methanol (solvent B), both containing 2.5 mmol/L of ammonium acetate, was adopted: 0–2 min, isocratic at 60% solvent B; 2–5 min, linear from 60 to 98% (*v*/*v*) of solvent B; 5–15 min, linear from 98 to 100% (*v*/*v*) of solvent B; 15–30 min, isocratic at 100% solvent B; 30–35 min, linear to 60% solvent B (initial composition) followed by 10 min equilibration time. The flow rate was 0.3 mL/min. MS full scan acquisitions were performed in negative ion mode, in the *m*/*z* range 50–2000. The following values were adopted for the heated ESI (HESI) interface (Thermo Scientific) and ion optics parameters: sheath gas flow rate, 35 (arbitrary units); auxiliary gas flow rate, 15 (arbitrary units); spray voltage, 3.5 kV (negative polarity); capillary temperature, 220 °C; and S-lens RF level, 68 (arbitrary units). MS/MS and MS^3 acquisitions were performed on target precursor ions. Only the M isotopologue of each precursor ion was isolated before fragmentation, using a 1 *m*/*z* wide window centred on its *m*/*z* ratio. The M+2 isotopologue was always excluded from isolation and fragmentation to avoid spectral interferences; indeed, the presence of partially co-eluting CL having 2 unit-spaced *m*/*z* ratios was not rare in the analysed samples. Normalized collisional energy for MS/MS and MS^3 was typically 35% (note that, in the case of the Velos Pro spectrometer, a 400% value for the normalized energy corresponds to 100-V excitation voltage). The control of the LC-MS instrumentation and the first processing of data were performed by the Xcalibur software 2.2 SP1.48 (Thermo Scientific). After the first processing, MS raw data were imported, further elaborated and finally turned into figures by the SigmaPlot 11.0 software (Systat Software, Inc., London, UK). The ChemDraw Pro 8.0.3 software (CambridgeSoft Corporation, Cambridge, MA, USA) was employed to draw chemical structures.

Growth of microorganisms and lipid extract preparation

R. sphaeroides R26 were grown under light exposure in anaerobic conditions, according to the procedure already described [33, 34]. Lipids were subsequently extracted from bacterial cells, using the Bligh-Dyer method [35] as previously reported [28]. Briefly, the lipid extracts were dissolved in chloroform (10 mg/mL) and 10 μL was applied onto a silica plate to perform a TLC separation [33]. Spots corresponding to CL were scratched off the TLC plate and lipids were extracted by vortexing the silica powder with a mixture of $CHCl_3/CH_3OH$ (1:1, *v*/*v*) (four times). After each addition, the organic layer was centrifuged (5000 rpm, 5 min) and the supernatant collected. Finally, the combined organic phases were evaporated to dryness and the residue was reconstituted in 200 μL of $CHCl_3/CH_3OH$ (1:1).

Results and discussion

Separation of CL by RPLC-ESI-MS

The TLC fraction containing CL of *R. sphaeroides* was analysed by reversed-phase liquid chromatography coupled to MS in negative polarity, thus exploiting the hydrophobicity of CL acyl chains for separation and the negative charge of one of their phosphate moieties for mass spectrometric detection. The main *m*/*z* ratios of deprotonated molecules (i.e. singly charged ions, $[M-H]^-$) retrieved from mass spectra averaged under the entire total ion current (TIC) chromatogram were used as inputs for a search based on the *online lipid calculator* database (http://www.mslipidomics.info/lipid-calc/), setting a tolerance of ±0.5 Da for each selected *m*/*z* value. By such an approach, 14 CL species differing for the overall number of carbon atoms and double bonds on their side chains were preliminarily identified (see Table 1). A representative chromatogram, obtained through multiple ion current extraction for the $[M-H]^-$ ions of the six most relevant CL species detected in the bacterial extracts, is reported in Fig. 1. As shown in the figure, the most abundant CL had a side chain composition 72:4 (*m*/*z* 1456.0) and was followed, in terms of MS signal intensity, by CL 72:3 (*m*/*z* 1458.0) and 66:3 (*m*/*z* 1373.9). Cardiolipins were detected mainly as mono-charged deprotonated species ($[M-H]^-$) [9], as clearly demonstrated by the relative abundance of peaks detected at *m*/*z* 1456.0 and 727.5 in the ESI-MS spectrum of Fig. 2, corresponding to the $[M-H]^-$ and the $[M-2H]^{2-}$ ions of CL 72:4, respectively (insets show their isotopic patterns). Likewise, mono-charged ions were detected at *m*/*z* 1478.0 and 1494.0, i.e. at values 22 and 38 units higher than the *m*/*z* value of the deprotonated molecule, demonstrating the formation of sodium ($[M-2H+Na]^-$) and potassium ($[M-2H+K]^-$) adducts, whose identity was subsequently confirmed by multistage CID-MS/MS experiments (see Section S1, Fig. S1 and Schemes S1/S2 in the Electronic supplementary material (ESM)). These adducts are likely generated by an internal charge compensation occurring during the ESI process, reasonably triggered by the presence of alkali metal ions as LC solvent impurities.

Table 1 Structural information related to the main cardiolipin isomers identified in the lipid extract of *R. sphaeroides* R26 by RPLC-ESI MS^n, detected mainly as deprotonated molecules ($[M-H]^-$). The regiochemical assignment is given in the last column, according to the notation explained in the text

Peak no.	Formula (M)	$[M-H]^-$ (*m*/*z*)	CL C:D	$[PA_1-H]^-$ (*m*/*z*)	$[PA_2-H]^-$ (*m*/*z*)	Isomers	$sn_1/sn_2/sn_1'/sn_2'$[a]
1	$C_{73}H_{136}O_{17}P_2$	1345.9	CL 64:3	699.5	589.4	*a*	18:1/18:1_18:1/10:0
				699.5	589.4	*b*	18:1/18:1_12:0/16:1
				671.5	617.4	*c*	16:1/18:1_18:1/12:0
2	$C_{73}H_{138}O_{17}P_2$	1347.9	CL 64:2	699.5	591.4	*a*	18:1/18:1_16:0/12:0
				673.5	617.4	*b*	18:1/16:0_18:1/12:0
3	$C_{73}H_{140}O_{17}P_2$	1349.9	CL 64:1	701.5	591.4	*a*	18:1/18:0_16:0/12:0
				673.5	619.4	*b*	18:1/16:0_18:0/12:0
				675.5	617.4	*c*	16:0/18:0_18:1/12:0
4	$C_{75}H_{140}O_{17}P_2$	1373.9	CL 66:3	699.5	617.4	*a*	18:1/18:1_18:1/12:0
5	$C_{75}H_{142}O_{17}P_2$	1376.0	CL 66:2	699.5	619.4	*a*	18:1/18:1_18:0/12:0
				701.5	617.5	*b*	18:0/18:1_18:1/12:0
6	$C_{75}H_{144}O_{17}P_2$	1378.0	CL 66:1	701.5	619.4	*a*	18:1/18:0_18:0/12:0
				703.5	617.4	*b*	18:0/18:0_18:1/12:0
7	$C_{77}H_{146}O_{17}P_2$	1404.0	CL 68:2	673.5	673.5	*a*	16:0/18:1_16:0/18:1
				647.5	699.5	*b*	16:0/16:0_18:1/18:1
				699.5	647.5	*c*	18:1/18:1_16:0/16:0
8	$C_{79}H_{146}O_{17}P_2$	1428.0	CL 70:4	699.5	671.5	*a*	18:1/18:1_18:1/16:1
9	$C_{79}H_{148}O_{17}P_2$	1430.0	CL 70:3	699.5	673.5	*a*	18:1/18:1_18:1/16:0
10	$C_{79}H_{150}O_{17}P_2$	1432.0	CL 70:2	673.5	701.5	*a*	18:1/16:0_18:1/18:0
				675.5	699.5	*b*	18:0/16:0_18:1/18:1
				675.5	699.5	*c*	17:0/17:0_18:1/18:1
11	$C_{80}H_{150}O_{17}P_2$	1444.0	CL 71:3	687.5	699.5	*a*	17:0/18:1_18:1/18:1
12[b]	$C_{81}H_{150}O_{17}P_2$	1456.0	CL 72:4	699.5	699.5	*a*	18:1/18:1/18:1/18:1
13	$C_{81}H_{152}O_{17}P_2$	1458.0	CL 72:3	699.5	701.5	*a*	18:1/18:1_18:1/18:0
14	$C_{81}H_{154}O_{17}P_2$	1460.0	CL 72:2	701.5	701.5	*a*	18:0/18:1/18:0/18:1
				699.5	703.5	*b*	18:1/18:1_18:0/18:0
				699.5	703.5	*c*	18:1/18:1–19:0/17:0

[a] Notation based on Liebisch et al. [30]

[b] The CL species detected at *m*/*z* 1456.0 was the most abundant in the lipid extracts of *R. sphaeroides* R26

The chromatographic separation achieved for individual CL can be better appreciated in Fig. 3, in which multiple extracted ion current (multi-XIC) chromatograms referred to species having the same overall number of carbon atoms, but differing just for one double bond, are reported (i.e. CL 66:3 vs. 66:2, CL 70:4 vs. 70:3 and CL 72:4 vs. 72:3). As it can be seen from each panel, such CL were well resolved, thus ruling out the risk of spectral interference between ions related to M and M+2 isotopologues of CL having *n* and *n*+1 C=C bonds, respectively. All the six species considered in Fig. 3 were well separated from each other, the only exception being represented by CL 70:3 and 72:4 (numbered as peaks 9 and 12 in Fig. 3 and Table 1). Nevertheless, the latter could be easily distinguished in the *m*/*z* domain, since they exhibit different *m*/*z* ratios (1430.0 vs. 1456.0). As expected for RPLC separations, the observed elution order reflected the different hydrophobicity conferred to CL by the length of the acyl chains.

Fragmentation patterns of CL species obtained by ESI-CID-MS^n

As emphasized in the inset of Fig. 1, the general CL structure is composed of a central glycerol backbone, covalently linked at its sn_1 and sn_3 positions (indicated as 1′ and 3′ in the figure) to a phosphatidic acid (PA) moiety (annotated as PA_1 and PA_2, respectively). In turn, each PA is characterized by a combination of acyl chains linked to both OH groups of its glycerol skeleton (i.e. on positions annotated as sn_1 and sn_2 for PA_1 and sn_1' and sn_2' for PA_2) [12, 30]. Despite the remarkable structural variability of CL, tandem MS spectra obtained under low-energy CID conditions can provide useful structural information. As an example, the main fragmentation pathways obtained for the $[M-H]^-$ ion related to the CL bearing four 18:1 acyl chains (the prevailing CL in *R. sphaeroides* R26) are reported in Scheme 1. Ions labelled as $[PA-H]^-$, $[PG-H-H_2O]^-$ and $[PGP-H-H_2O]^-$ (where PA, PG and PGP stand for phosphatidic acid,

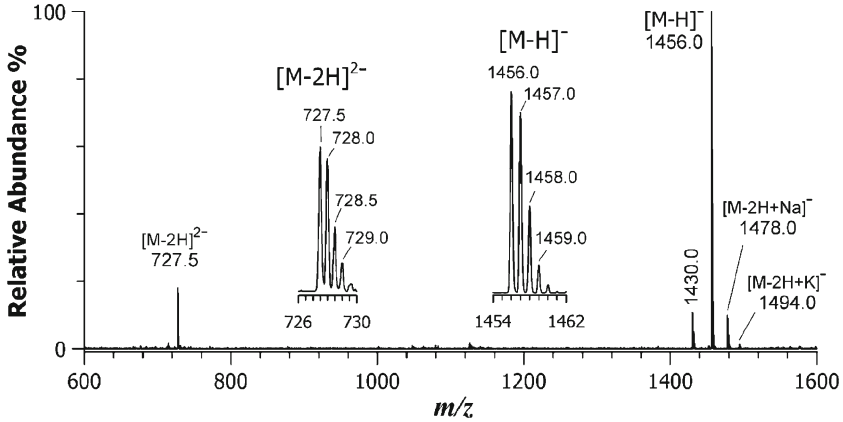

Fig. 2 ESI(−)MS spectrum obtained by spectral averaging in the time interval where elution of the most abundant CL 72:4 occurs (see Fig. 1). The generation of the doubly charged ion, at *m/z* 727.5 ($[M-2H]^{2-}$), and of three different singly charged ions, at *m/z* 1456.0 ($[M-H]^-$), 1478.0 ($[M-2H+Na]^-$) and 1494.0 ($[M-2H+K]^-$) is emphasized. Isotopic patterns obtained for $[M-2H]^{2-}$ and $[M-H]^-$ ions are shown in the *insets*

phosphatidylglycerol and phosphatidylglycerolphosphate, respectively) are generated from CL. These fragments imply the neutral loss of (*i*) a PG unit deprived of water, (*ii*) a PA unit and (*iii*) a diacyl-glycerol (DAG), respectively, as emphasized in Scheme 1. Additional product ions reported in the same scheme are consistent with the loss of a single acyl chain as fatty acid straight from the precursor ion and as fatty acid or as ketene from the $[PA-H]^-$ ion.

The CL fragmentation pattern becomes even more complex when species bearing acyl chains with different compositions are considered. In this case, once the central glycerol is taken as a reference, product ions including the PA unit linked

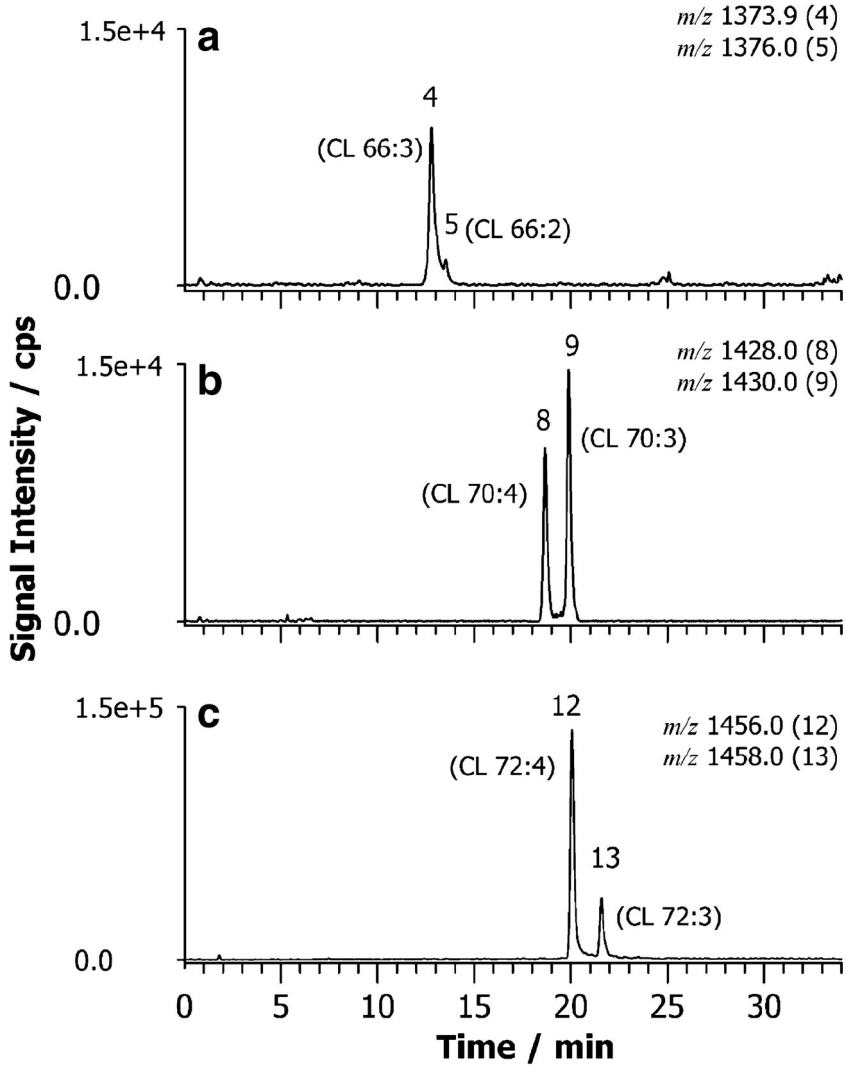

Fig. 3 **a**–**c** Extracted ion current (XIC) chromatograms of some CL species, as $[M-H]^-$ ions, obtained by RPLC-ESI-MS of *R. sphaeroides* R26 lipid extracts. Each XIC chromatogram was obtained using a 1 *m/z* unit wide window centred on the selected *m/z* values. Peaks are numbered as in Table 1

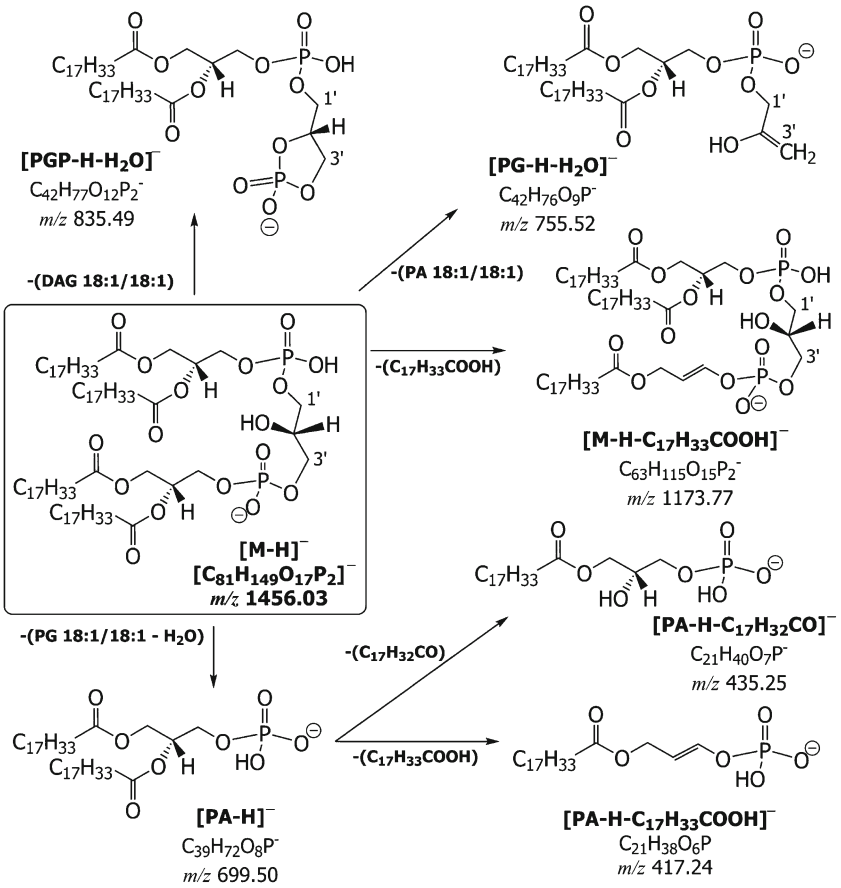

Scheme 1 Fragmentation pathways inferred from the low-energy CID MS/MS analysis of the $[M-H]^-$ ion of the cardiolipin 72:4 isomer corresponding to CL $(18:1)_4$, taken as a representative of the CL class in *R. sphaeroides* being the most abundant CL species in the bacterial extracts

to its 1′ position can be indicated by the subscript 1, i.e. $[PA_1\text{-}H]^-$, $[PG_1\text{-}H\text{-}H_2O]^-$ and $[PGP_1\text{-}H\text{-}H_2O]^-$, whereas those including the PA unit linked to the 3′ position can be marked with the subscript 2, i.e. $[PA_2\text{-}H]^-$, $[PG_2\text{-}H\text{-}H_2O]^-$ and $[PGP_2\text{-}H\text{-}H_2O]^-$ [12, 36]. As an example, Fig. 4a shows the CID-MS/MS spectrum of CL 72:3 (see peak 13 in Table 1), obtained by fragmenting the $[M-H]^-$ ion detected at *m/z* 1458.0. In this case, the main product ions, detected at *m/z* 669.5 and 701.5, corresponded to deprotonated PA 36:2 and PA 36:1, respectively. As emphasized in the inset of Fig. 4a, the peak at *m/z* 669.5 was slightly more abundant than the 701.5 one. Notably, the signal intensity ratio observed for $[PA-H]^-$ ions obtained upon fragmentation of a CL has been proposed as a diagnostic criterium to infer the location of the PA units in its structure [37]: the abundance order being $[PA_1\text{-}H]^- > [PA_2\text{-}H]^-$. Consequently, data shown in Fig. 4a suggest that the CL 72:3 isomer found in the lipid extracts of *R. sphaeroides* is predominantly, even not exclusively, characterized by PA_1 and PA_2 units with compositions 36:2 and 36:1, respectively. Considering that the $[PA_1\text{-}H]^-/[PA_2\text{-}H]^-$ intensity ratio was greater but close to unity, the presence of a small amount of isomeric CL with an inverse disposition of PA units cannot be ruled out (see notation used in Table 1).

To identify the location of acyl chains on both PA moieties, thus obtaining a more refined structural characterization, CID-MS^3 spectra of ions detected at *m/z* 669.5 and 701.5 were acquired. As suggested by the comparison of panels a and c in Fig. 4, the resulting MS^3 spectra showed very similar patterns, typical of the fragmentation of a PA in negative polarity [36, 38]. Therefore, two peaks or couples of peaks, corresponding to the neutral losses of acyl chains as fatty acids ($[PA\text{-}H\text{-}R_xCOOH]^-$ ions, detected at nominal *m/z* 417 and 419) or ketenes ($[PA\text{-}H\text{-}R_x'CH_2{=}C{=}O]^-$ ions, detected at nominal *m/z* 435 and 437) were observed. Relevant signals related to the detachment of PA unit side chains as carboxylate anions (nominal *m/z* 281 and 283) were also observed. According to literature data [12, 38, 39], the loss of side chains as fatty acids was prevailing over the loss as ketenes. Remarkably, weak signals due to $[PA\text{-}H\text{-}R_xCOOH]^-$ ions at *m/z* 417.2 and 435.2 were detected already in the MS/MS spectrum (see Fig. 4a).

The number and the *m/z* values of peaks detected in Fig. 4b clearly indicated the presence of two 18:1 chains on PA_1, since only one signal was detected for each possible fragmentation pathway, namely at *m/z* 417.3 and 435.3, representing the neutral losses of an octadecenoic acid (18:1) ($[PA\text{-}H\text{-}C_{17}H_{33}COOH]^-$) and the corresponding ketene species ($[PA\text{-}H\text{-}C_{16}H_{30}CH_2{=}C{=}O]^-$), respectively, and at *m/z* 281.2, corresponding to an octadecenoate anion ($[C_{17}H_{33}COO]^-$). As emphasized in Fig. 4c, the fragmentation, under MS^3 conditions, of the *m/z* 701.5 ion, i.e. of the $[PA_2(36:1)\text{-}H]^-$ ion, led to two signals for each type of

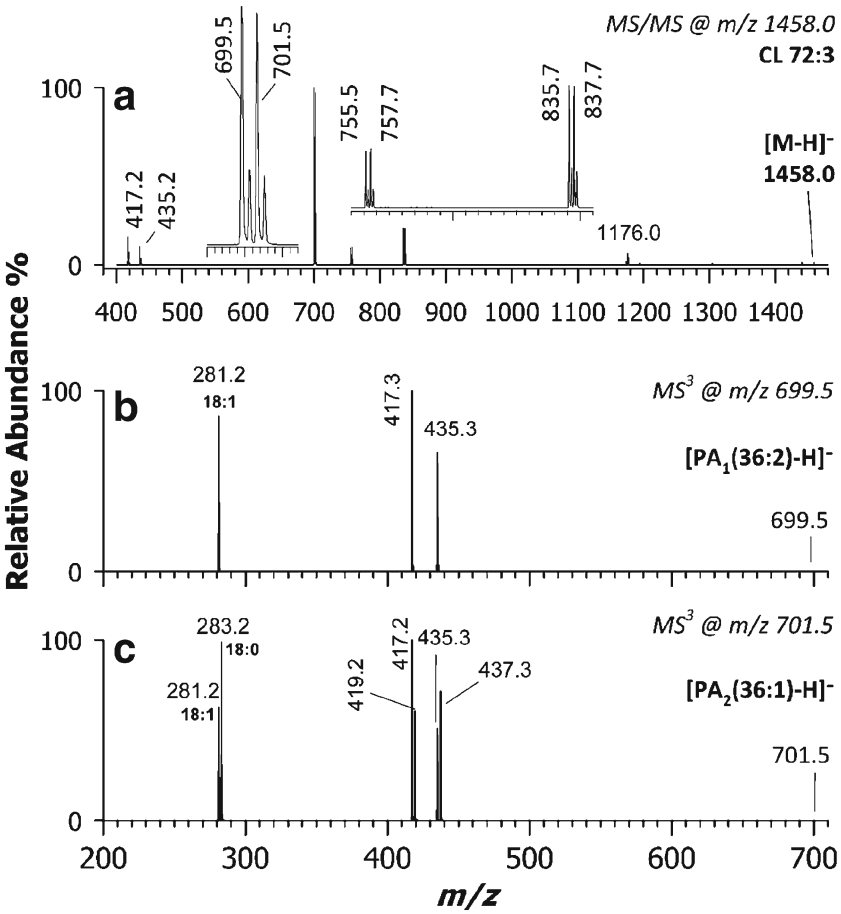

Fig. 4 ESI-MS/MS and MS^3 spectra obtained for CL 72:3 (18:1/18:1_18:1/18:0) detected in the lipid extracts of *R. sphaeroides* R26. **a**) MS/MS spectrum of the peak at *m/z* 1458.0, recognized as the $[M-H]^-$ ion. The *insets* show the enlargements of the *m/z* ranges 695–707 and 750–845, where diagnostic ions were detected. The less abundant ions correspond to $[PG\text{-}H\text{-}H_2O]^-$ (*m/z* 755.5 and 757.7) and $[PGP\text{-}H\text{-}H_2O]^-$ (*m/z* 835.7 and 837.7), whose structures are reported in Scheme 1. **b**) MS^3 spectrum of the PA ion presumably derived from the 1′ subunit of CL 72:3 at *m/z* 699.5, i.e. the most intense peak obtained in the MS/MS spectrum at *m/z* 1458.0. **c**) MS^3 spectrum obtained for the *m/z* 701.5 ion, i.e. the PA ion derived from the 3′ subunit of CL 72:3. See text for a detailed description of all product ions. Normalized collisional energy used 35%

product ion, highlighting the presence of two different acyl chains, having compositions 18:1 and 18:0. According to the *charge-driven-fragmentation* mechanism invoked for glycerophospholipid fragmentation [36, 38], the loss as fatty acid is favoured for the side chain linked to the sn_2 position of glycerol in the case of a PA [37]. Since the intensity ratio observed for signals related to the losses of 18:0 (*m/z* 417.2) and 18:1 (*m/z* 419.2) fatty acids was significantly higher than unity, a 18:1/18:0 composition, reported according to the sn_1/sn_2 regiochemical notation proposed by Liebisch et al. [30], was inferred as the prevailing one for the PA_2 (36:1).

Using the conventional regiochemical notation for CL, reporting the four side chain (C:D) compositions in the order sn_1, sn_2, sn'_1, sn'_2, with the first two related to the PA_1 unit and the last two to the PA_2 one, the CL 72:3 detected in *R. sphaeroides* could be finally annotated as CL 18:1/18:1_18:1/18:0 (see peak no. 13 in Table 1). The results shown in Fig. 4 and described above emphasize the key role played by MS^3 in the characterization of a CL at the level of the single PA units, since only the fragmentation under MS^3 conditions of $[PA\text{-}H]^-$ ions detected in the MS/MS spectrum of a CL $[M-H]^-$ ion can provide indications on the location of the two acyl chains on each PA unit.

CID-MS^n of isomeric CL

Intriguing results were obtained from the combination of CID-MS/MS and MS^3 analyses of CL with two, or even three, different isomers occurring in the lipid extracts of *R. sphaeroides* R26. As an example, the tandem MS spectrum of the ion detected at *m/z* 1376.0 (peak 5 in Table 1), corresponding to CL 66:2, is reported in Fig. 5a. The *m/z* scale expansion, reported in panel a, clearly emphasizes the existence of four peaks due to $[PA\text{-}H]^-$ ions, namely those detected at *m/z* 617.4 (PA 30:1), 619.4 (PA 30:0), 699.5 (PA 36:2) and 701.5 (PA 36:1), accompanied by as many ions related to each of the other fragmentation pathways described in Scheme 1. This finding clearly suggested the occurrence of two isomeric CL 66:2 species differing at the level of their PA units. Following the same approach discussed before, based on relative abundances of $[PA\text{-}H]^-$ ions, the predominant PA_1/PA_2 compositions of the two CL 66:2 isomers could be inferred as 36:1/30:1 and 36:2/30:0 because the 701.5/617.4 and 699.5/619.4 intensity ratios were both slightly greater than 1, as shown in Fig. 5a. A confirmation of the presence of two distinct CL species was retrieved by MS^3 experiments, i.e. by fragmentation of each of the four $[PA\text{-}H]^-$ ions detected in the MS/MS spectrum. As shown in Fig. 5b, the precursor ion at *m/z* 617.4 generates two product ions at *m/z* 417.3 and 335.2,

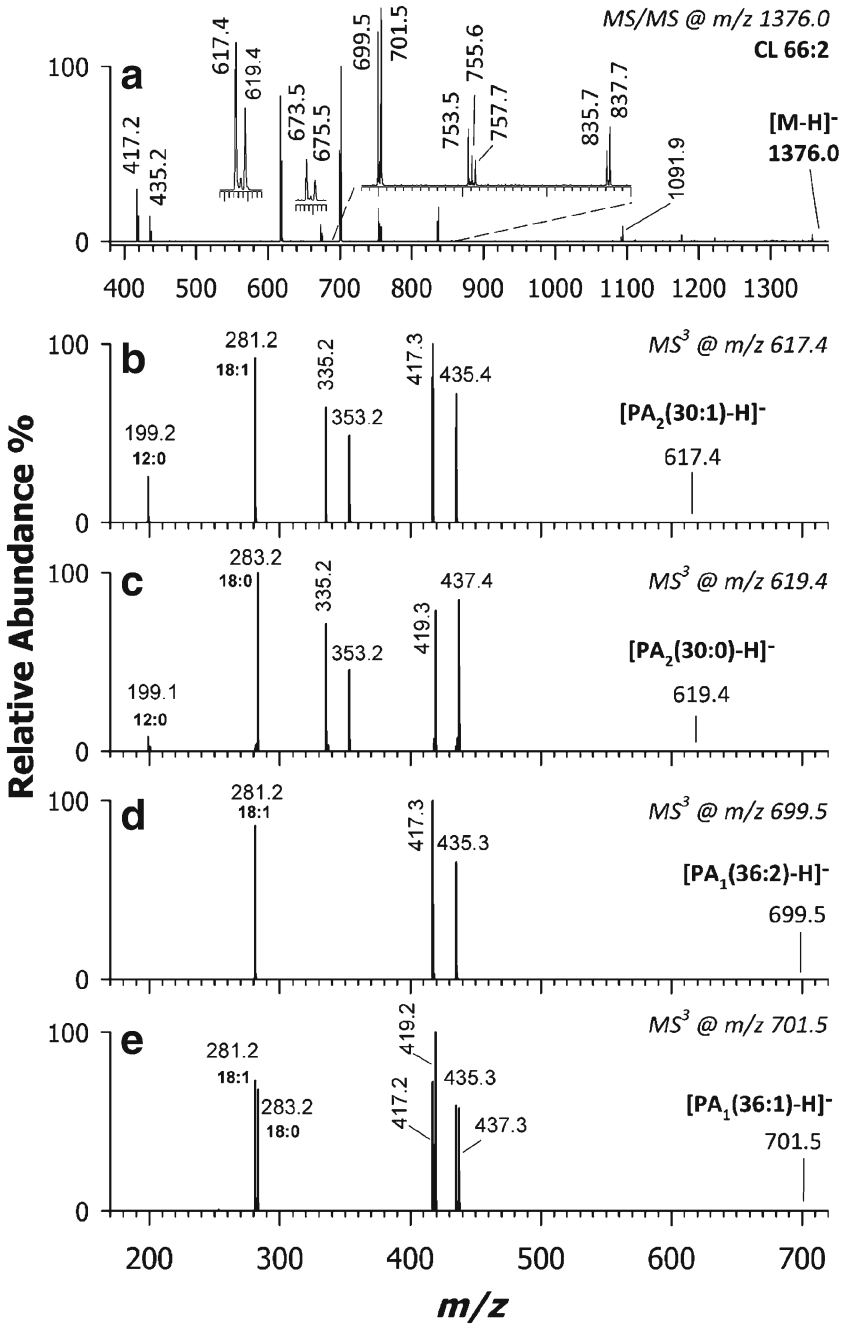

Fig. 5 ESI-MS/MS and MS^3 spectra obtained for CL 66:2 (peak 5 in Table 1) detected in the lipid extracts of *R. sphaeroides* R26. **a**) MS/MS spectrum of the peak at *m/z* 1376.0, recognized as the $[M-H]^-$ ion. The *inset* shows an enlargement of the *m/z* range 680–850, where diagnostic ions were detected. **b**) MS^3 spectrum of the peak at *m/z* 617.4. **c**) MS^3 spectrum of the peak at *m/z* 619.4. **d**) MS^3 spectrum of the peak at *m/z* 699.5. **e**) MS^3 spectrum of the peak at *m/z* 701.5. See text for a detailed description of all the detected product ions. Normalized collisional energy used 35%

which could be interpreted as the neutral losses as fatty acids 12:0 and 18:1, respectively. In this case, the prevailing peak was the one related to the loss of the 12:0 chain; thus, the 18:1/12:0 regiochemistry could be inferred as the prevailing one. Using the same approach, peaks detected at *m/z* 619.4, 699.5 and 701.5 in the MS/MS spectrum of Fig. 5a could be assigned as PA 18:0/12:0, 18:1/18:1 and 18:0/18:1, respectively. As a result, the presence of two prevailing, co-eluting CL 66:2 species, corresponding to compositional isomers 18:0/18:1_18:1/12:0 (species 5b in Table 1) and CL 18:1/18:1_18:0/12:0 (species 5a in Table 1), was successfully established in the lipid extracts of *R. sphaeroides*.

Another valuable example of multistage CID-MS characterization performed on isomeric CL refers to CL 70:2 (peak 10 in Table 1), detected as $[M-H]^-$ ion at *m/z* 1432.0. The corresponding MS/MS spectrum, reported in Fig. 6a, exhibited four $[PA-H]^-$ signals, at *m/z* 673.5, 675.5, 699.5 and 701.5, demonstrating the occurrence of four PA units with side chain compositions 34:1, 34:0, 36:2 and 36:1, respectively. The evaluation of the relative abundances of $[PA-H]^-$ ions suggested that the 1′ and 3′ positions of the central glycerol were linked to PA 34:1 and PA 36:1, respectively, in one of the CL 70:2 isomers, namely the most abundant one (see the prevalence of *m/z* 673.5 and 701.5 ions over those detected at *m/z*

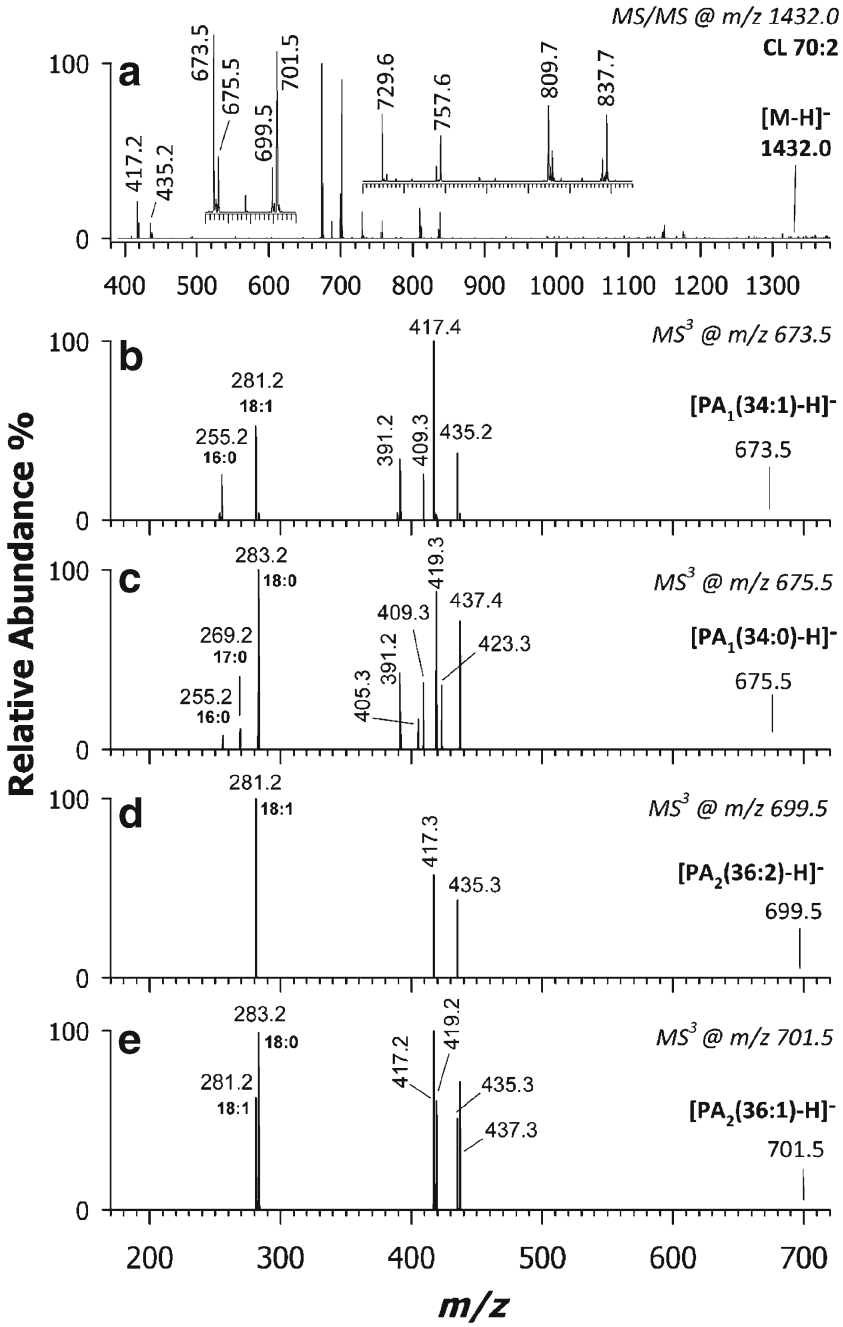

Fig. 6 ESI-MS/MS and MS^3 spectra obtained for CL 70:2 (peak 10 in Table 1) detected in the lipid extracts of *R. sphaeroides* R26. **a**) MS/MS spectrum of the peak at *m/z* 1432.0, recognized as the $[M-H]^-$ ion. The *insets* show two enlargements of *m/z* range 670–900, where diagnostic ions were detected. **b**) MS^3 spectrum of the peak at *m/z* 673.5. **c**) MS^3 spectrum of the peak at *m/z* 675.5. **d**) MS^3 spectrum of the peak at *m/z* 699.5. **e**) MS^3 spectrum of the peak at *m/z* 701.5. See text for a detailed description of all the detected product ions. Normalized collisional energy used 35%

675.5 and 699.5). The other isomer was characterized by the presence of PA 34:0 and PA 36:2 on the 1′ and 3′ positions, respectively. In both cases, isomeric CL bearing the PA units on inverse positions of the central glycerol molecule could be present, although with lower amounts, since both the 673.5/701.5 and the 675.5/699.5 intensity ratios were only slightly greater than unity.

The MS^3 spectrum arising from the fragmentation of the precursor ion at *m/z* 673.5 (see Fig. 6b) led to the identification of PA 34:1 (*m/z* 673.5) as a PA 18:1/16:0 (indeed, the intensity ratio 417.4/391.2, related to fatty acids losses, was greater than 3). The PA 36:1 moiety (*m/z* 701.5) was recognized to be a PA 18:1/18:0 (see Fig. 6e). Consequently, the main isomer of CL 70:2 was found to correspond to CL 18:1/16:0_18:1/18:0 (i.e. peak 10a in Table 1). As for the *m/z* 675.5 ion, the co-existence of two isomeric PA 34:0 ions was inferred from the MS^3 fragmentation; indeed, three neutral losses of side chains as fatty acids, namely 16:0 ($[PA\text{-}H\text{-}C_{15}H_{31}COOH]^-$ at *m/z* 419.3), 18:0 ($[PA\text{-}H\text{-}C_{17}H_{35}COOH]^-$ at *m/z* 391.2) and 17:0 ($[PA\text{-}H\text{-}C_{16}H_{33}COOH]^-$ at *m/z* 405.3), were observed (see Fig. 6c). Starting from the overall side chain composition and from the number and relative intensity of signals due to fatty acid losses, the regiochemical compositions of the two possible PA 34:0 units were recognized as

18:0/16:0 and 17:0/17:0. Finally, the ion at *m/z* 699.5 was recognized as PA 18:1/18:1 (see Fig. 6d). Consequently, the presence of two additional CL 70:2 isomers, whose compositions can be annotated as 18:0/16:0_18:1/18:1 and 17:0/17:0_18:1/18:1, peak 10b and 10c, respectively, was ascertained.

A further interesting case of distinction between isomeric CL is represented by the characterization of CL 72:2 (peak 14 in Table 1), whose $[M-H]^-$ ion was detected at *m/z* 1460.0 (see Fig. 7). The relevant MS/MS spectrum (Fig. 7a) showed signals for three $[PA-H]^-$ ions, at *m/z* 701.5 (PA 36:1, the prevailing one), 699.5 (PA 36:2) and 703.5 (PA 36:0). The subsequent fragmentation, under MS^3 conditions, of the peak at *m/z* 701.5 enabled its identification as a PA 18:0/18:1 (see Fig. 7c), thus suggesting that the main isomer of CL 72:2 in *R. sphaeroides* lipid extracts was a CL 18:0/18:1/18:0/18:1. Considering the whole composition of side chains, the other two detected PA units could be clearly related to the presence of at least another CL 72:2 isomer. However, while the MS^3 fragmentation of the *m/z* 699.5 ion enabled its identification as PA 18:1/18:1 (see plot b in Fig. 7), the one obtained from the *m/z* 703.5 ion revealed the presence of two isobaric $[PA-H]^-$ ions, namely a 18:0/18:0 (with losses of a 18:0 fatty acids leading to the *m/z* 419.2 ion) and a rather unusual 19:0/17:0 (with the loss of the 17:0 fatty acid, corresponding to the *m/z* 433.2 ion, being remarkably more likely than that of the 19:0 acid, corresponding to the *m/z* 405.2 ion; see plot d of Fig. 7). Hence, also CL 72:2 appeared to correspond to three co-eluting isomers as peaks 14a, 14b and 14c, i.e. 18:0/18:1/18:0/18:1, 18:1/18:1_18:0/18:0 and 18:1/18:1_19:0/17:0, respectively.

As evidenced in Table 1, two or three main isomers were identified for many of the 14 CL compositions identified in the lipid extracts of *R. sphaeroides*, leading to a total of 27 CL species. The presence of minor CL with reversed PA units and/or reversed regiochemistry on a specific PA unit,

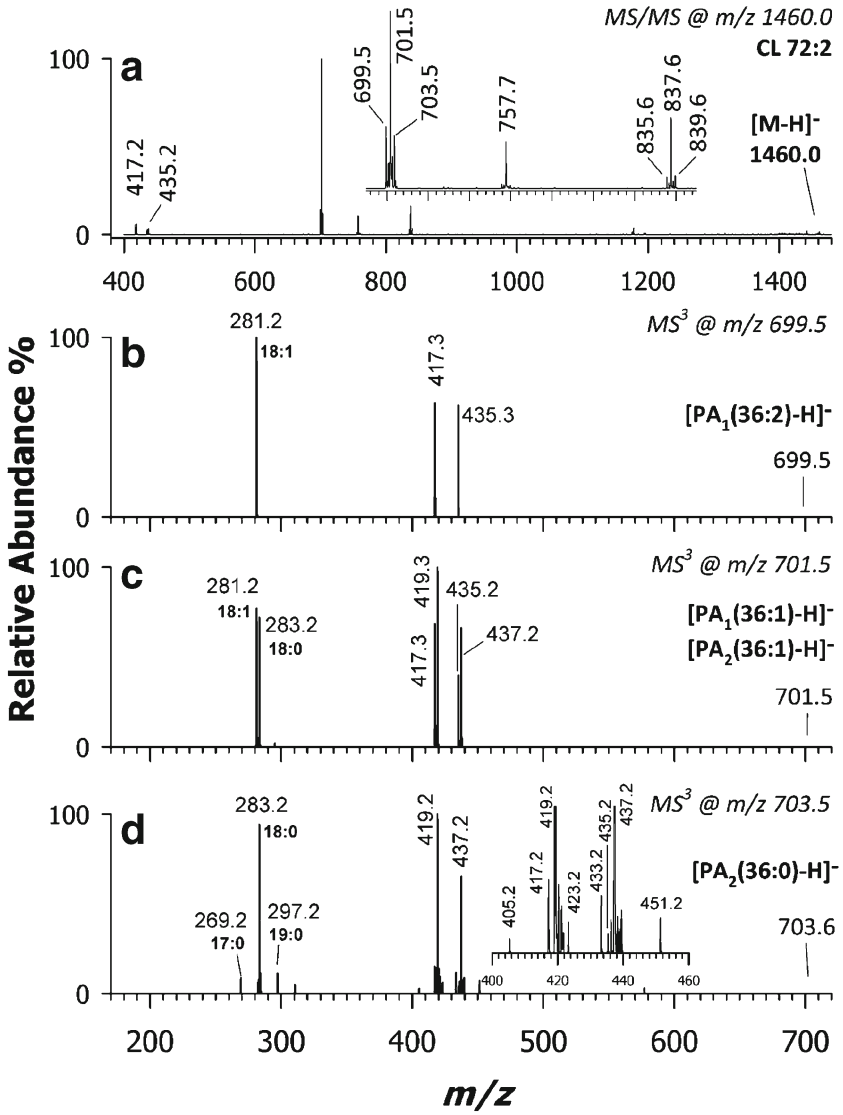

Fig. 7 ESI-MS/MS and MS^3 spectra obtained for CL 72:2 (peak 14 in Table 1) detected in the lipid extracts of *R. sphaeroides* R26. **a**) MS/MS spectrum of the peak at *m/z* 1460.0, recognized as the $[M-H]^-$ ion. The *inset* shows an enlargement of *m/z* range 665–845, where diagnostic ions were detected. **b**) MS^3 spectrum of the peak at *m/z* 699.5. **c**) MS^3 spectrum of the peak at *m/z* 701.5. **d**) MS^3 spectrum of the peak at *m/z* 703.6. See text for a detailed description of all the detected product ions. Normalized collisional energy 35%

compared to their major counterparts, was often inferred from MS/MS and MS^3 data. The set of species reported in Table 1 represents a much more refined characterization of the CL profile in *R. sphaeroides*, compared to the one reported before in the literature, based just on four CL, those with global chain compositions 70:3, 70:4, 72:3 and 72:4. Additional considerations are deserved by the definite nature of the acyl chains recognized in the CL species of *R. sphaeroides* R26. Specifically, only saturated (i.e. 12:0, 16:0, 17:0, 18:0, 19:0) or mono-unsaturated (i.e. 16:1 and 18:1) acyl chains were found, whereas the 18:2 chain, constituting the leading CL, $(18:2)_4$, found in the mitochondria of mammalian and higher plant cells, was missing. Instead, the 12:0 chain found in many *R. sphaeroides* R26 CL was also reported for CL of yeast [40] and *Escherichia coli* [41].

The differences in the CL profile may indicate well-definite differences in the functional role that these lipids play in bacteria and yeasts [29], compared to mammals. Indeed, 18:2 chains present in mammalian CL allow peroxidation reactions, in turn functional to signalling related to apoptosis, in which CL are involved. Furthermore, bacteria do not include the acyltransferase enzyme, required to obtain a CL $(18:2)_4$ [29]. The limited number of double bonds found in the structures of CL identified in *R. sphaeroides*, never exceeding four, is consistent with the lack of polyunsaturated fatty acids observed in previous studies on the same bacterium [33, 42]. This feature suggests a high oxidative stability of *R. sphaeroides* R26 membranes, which may be useful to overcome the absence of carotenoids in this mutant. Although acyl chains with an even number of carbon atoms were prevailing in the CL of *R. sphaeroides* R26, odd-numbered chains, like 17:0 and 19:0, were also observed among saturated ones, in accordance with previous studies [42, 43]. Interestingly, such acyl chains have been also found during a recent investigation on the ornithine lipids of the same bacterium [33]. Odd-numbered chains perhaps correspond to branched fatty acids, in particular to methylated form of typical even numbered chains, whose main function in bacterial CL might be increasing the fluidity of cell membranes, as an alternative to chains bearing one or more *cis* double bonds, which are more liable to chemical oxidation.

Conclusions

The present study has highlighted the effectiveness of a multistage CID-MS-based approach, in conjunction with RPLC, for an extended characterization of CL in the lipid extracts of the bacterium *R. sphaeroides* R26. An unprecedented number of different main CL (i.e. 27) was identified, many of them representing compositional or regiochemical isomers resulting from the combination of a relatively small number of different acyl chains. The presence of minor isomeric CL with reversed order of PA units was also inferred; acyl chains of the detected CL were either saturated or mono-unsaturated, a feature that may be related to the need of *R. sphaeroides* R26 to protect its membrane from oxidative stress in the absence of defence mechanisms as those related to carotenoid pigments, lacking in that strain. The refined structural characterization of bacterial CL enabled by multistage MS analyses appears then a promising approach in the perspective of studying, through CL composition, further important aspects of bacterial biology, like the response to osmotic stresses or, in the case of photosynthetic bacteria, the effect of CL depletion on the functioning of reaction centres.

Acknowledgements We would like to thank the anonymous reviewer for her/his recommendation on the acyl combination of the PA units. This work was supported by the project PONa3_00395/1 "BIOSCIENZE & SALUTE (B&H)" of Italian Ministero per l'Istruzione, l'Università e la Ricerca (MIUR). Dr. V. De Leo and Dr. F. Italiano are acknowledged for their help in the preparation of bacterial extracts.

Compliance with ethical standards

Conflict of interest The authors declare that they have no conflict of interest.

References

1. Schlame M. Cardiolipin synthesis for the assembly of bacterial and mitochondrial membranes. J Lipid Res. 2008;49:1607–20. doi:10.1194/jlr.R700018-JLR200.
2. Haines TH. A new look at cardiolipin. Biochim Biophys Acta-Biomembr. 2009;1788:1997–2002. doi:10.1016/j.bbamem.2009.09.008.
3. Claypool SM, Koehler CM. The complexity of cardiolipin in health and disease. Trends Biochem Sci. 2012;37:32–41. doi:10.1016/j.tibs.2011.09.003.
4. Scherer M, Schmitz G, Liebisch G. Simultaneous quantification of cardiolipin, bis(monoacylglycero)phosphate and their precursors by hydrophilic interaction LC-MS/MS including correction of isotopic overlap. Anal Chem. 2010;82:8794–9. doi:10.1021/ac1021826.
5. Bowron A, Frost R, Powers VEC, Thomas PH, Heales SJR, Steward CG. Diagnosis of Barth syndrome using a novel LC-MS/MS method for leukocyte cardiolipin analysis. J Inherit Metab Dis. 2013;36:741–6. doi:10.1007/s10545-012-9552-4.
6. Xu Y, Phoon CKL, Berno B, D'Souza K, Hoedt E, Zhang G, et al. Loss of protein association causes cardiolipin degradation in Barth syndrome. Nat Chem Biol. 2016;12:641–7. doi:10.1038/nCHeMBIO.2113.
7. Tyurina YY, Polimova AM, Maciel E, Tyurin VA, Kapralova VI, Winnica DE, et al. LC/MS analysis of cardiolipins in substantia nigra and plasma of rotenone-treated rats: implication for mitochondrial dysfunction in Parkinson's disease. Free Radic Res. 2015;49:681–91. doi:10.3109/10715762.2015.1005085.
8. Okazaki Y, Kamide Y, Hirai MY, Saito K. Plant lipidomics based on hydrophilic interaction chromatography coupled to ion trap time-of-flight mass spectrometry. Metabolomics. 2013;9:121–31. doi:10.1007/s11306-011-0318-z.
9. Zhou Y, Peisker H, Dörmann P. Molecular species composition of plant cardiolipin determined by liquid chromatography mass spectrometry. J Lipid Res. 2016;57:1308–21. doi:10.1194/jlr.D068429.

10. Bird SS, Marur VR, Sniatynski MJ, Greenberg HK, Kristal BS. Lipidomics profiling by high-resolution LC-MS and high-energy collisional dissociation fragmentation: focus on characterization of mitochondrial cardiolipins and monolysocardiolipins. Anal Chem. 2011;83:940–9. doi:10.1021/ac102598u.
11. Minkler PE, Hoppel CL. Separation and characterization of cardiolipin molecular species by reverse-phase ion pair high-performance liquid chromatography-mass spectrometry. J Lipid Res. 2010;51:856–65. doi:10.1194/jlr.D002857.
12. Garrett TA, Kordestani R, Raetz CRH. Quantification of cardiolipin by liquid chromatography-electrospray ionization mass spectrometry. Methods Enzymol. 2007;433:213–30.
13. Maciel E, Domingues P, Domingues MRM. Liquid chromatography/tandem mass spectrometry analysis of long-chain oxidation products of cardiolipin induced by the hydroxyl radical. Rapid Commun Mass Spectrom. 2011;25:316–26. doi:10.1002/rcm.4866.
14. De Leo V, Catucci L, Ventrella A, Milano F, Agostiano A, Corcelli A. Cardiolipin increases in chromatophores isolated from Rhodobacter sphaeroides after osmotic stress: structural and functional roles. J Lipid Res. 2009;50:256–64. doi:10.1194/jlr.M800312-JLR200.
15. McAuley KE, Fyfe PK, Ridge JP, Isaacs NW, Cogdell RJ, Jones MR. Structural details of an interaction between cardiolipin and an integral membrane protein. Proc Natl Acad Sci U S A. 1999;96:14706–11. doi:10.1073/pnas.96.26.14706.
16. Catucci L, Depalo N, Lattanzio VMT, Agostiano A, Corcelli A. Neosynthesis of cardiolipin in Rhodobacter sphaeroides under osmotic stress. Biochemistry. 2004;43:15066–72. doi:10.1021/bi048802k.
17. Mackenzie C, Eraso JM, Choudhary M, Roh JH, Zeng X, Bruscella P, et al. Postgenomic adventures with Rhodobacter sphaeroides. Annu Rev Microbiol. 2007;61:283–307. doi:10.1146/annurev.micro.61.080706.093402.
18. Cox JC, Madigan MT, Favinger JL, Gest H. Redox mechanisms in "oxidant-dependent" hexose fermentation by Rhodopseudomonas capsulata. Arch Biochem Biophys. 1980;204:10–7. doi:10.1016/0003-9861(80)90002-8.
19. Madigan MT, Gest H. Growth of a photosynthetic bacterium anaerobically in darkness, supported by "oxidant-dependent" sugar fermentation. Arch Microbiol. 1978;117:119–22. doi:10.1007/BF00402298.
20. Yen HC, Marrs B. Growth of Rhodopseudomonas capsulata under anaerobic dark conditions with dimethyl sulfoxide. Arch Biochem Biophys. 1977;181:411–8. doi:10.1016/0003-9861(77)90246-6.
21. Kiley PJ, Kaplan S. Molecular genetics of photosynthetic membrane biosynthesis in Rhodobacter sphaeroides. Microbiol Rev. 1988;52:50–69.
22. Schultz JE, Weaver PF. Fermentation and anaerobic respiration by Rhodospirillum rubrum and Rhodopseudomonas capsulata. J Bacteriol. 1982;149:181–90.
23. Sardaro A, Castagnolo M, Trotta M, Italiano F, Milano F, Cosma P, et al. Isothermal microcalorimetry of the metabolically versatile bacterium Rhodobacter sphaeroides. J Therm Anal Calorim. 2013;112:505–11. doi:10.1007/s10973-012-2895-0.
24. Sistrom WR, Clayton RK. Studies on a mutant of Rhodopseudomonas spheroides unable to grow photosynthetically. Biochim Biophys Acta. 1964;88:61–73. doi:10.1016/0926-6577(64)90154-8.
25. Clayton RK, Smith C. Rhodopseudomonas sphaeroides: high catalase and blue-green double mutants. Biochem Biophys Res Commun. 1960;3:143–5. doi:10.1016/0006-291X(60)90210-2.
26. Cogdell RJ, Crofts AR. Analysis of the pigment content of an antenna pigment-protein complex from three strains of Rhodopseudomonas sphaeroides. BBA-Bioenerg. 1978;502:409–16. doi:10.1016/0005-2728(78)90074-9.
27. Italiano F, Buccolieri A, Giotta L, Agostiano A, Valli L, Milano F, et al. Response of the carotenoidless mutant Rhodobacter sphaeroides growing cells to cobalt and nickel exposure. Int Biodeterior Biodegrad. 2009;63:948–57. doi:10.1016/j.ibiod.2009.05.001.
28. Calvano CD, Italiano F, Catucci L, Agostiano A, Cataldi TRI, Palmisano F, et al. The lipidome of the photosynthetic bacterium Rhodobacter sphaeroides R26 is affected by cobalt and chromate ions stress. Biometals. 2014;27:65–73. doi:10.1007/s10534-013-9687-2.
29. Zhang X, Tamot B, Hiser C, Reid GE, Benning C, Ferguson-Miller S. Cardiolipin deficiency in Rhodobacter sphaeroides alters the lipid profile of membranes and of crystallized cytochrome oxidase, but structure and function are maintained. Biochemistry. 2011;50:3879–90. doi:10.1021/bi101702c.
30. Liebisch G, Vizcaino JA, Kofeler H, Trotzmuller M, Griffiths WJ, Schmitz G, et al. Shorthand notation for lipid structures derived from mass spectrometry. J Lipid Res. 2013;54:1523–30. doi:10.1194/jlr.M033506.
31. Douglas DJ, Frank AJ, Mao D. Linear ion traps in mass spectrometry. Mass Spectrom Rev. 2005;24:1–29. doi:10.1002/mas.20004.
32. Remaut H, Fronzes R. Bacterial membranes: structural and molecular biology. Norfolk: Caister Academic Press; 2014.
33. Granafei S, Losito I, Trotta M, Italiano F, de Leo V, Agostiano A, et al. Profiling of ornithine lipids in bacterial extracts of Rhodobacter sphaeroides by reversed-phase liquid chromatography with electrospray ionization and multistage mass spectrometry (RPLC-ESI-MSn). Anal Chim Acta. 2016;903:110–20. doi:10.1016/j.aca.2015.11.020.
34. Buccolieri A, Italiano F, Dell'Atti A, Buccolieri G, Giotta L, Agostiano A, et al. Testing the photosynthetic bacterium Rhodobacter sphaeroides as heavy metal removal tool. Ann Chim. 2006;96:195–203.
35. Bligh EG, Dyer WJ. A rapid mathod of total lipid extraction and purification. Can J Biochem Physiol. 1959;37:911–7. doi:10.1139/o59-099.
36. Han X. Lipidomics comprehensive mass spectrometry of lipids, June 2016. Wiley Ser Mass Spectrom. 2016; doi:10.1088/1751-8113/44/8/085201.
37. Hsu F-F, Turk J, Rhoades ER, Russell DG, Shi Y, Groisman EA. Structural characterization of cardiolipin by tandem quadrupole and multiple-stage quadrupole ion-trap mass spectrometry with electrospray ionization. J Am Soc Mass Spectrom. 2005;16:491–504. doi:10.1016/j.jasms.2004.12.015.
38. Murphy RC. Tandem mass spectrometry of lipids: molecular analysis of complex lipids. London: Royal Society of Chemistry; 2015. doi:10.1039/9781782626350.
39. Pulfer M, Murphy RC. Electrospray mass spectrometry of phospholipids. Mass Spectrom Rev. 2003;22:332–64. doi:10.1002/mas.10061.
40. Rattray JB, Schibeci A, Kidby DK. Lipids of yeasts. Bacteriol Rev. 1975;39:197–231.
41. Garrett TA, O'Neill AC, Hopson ML. Quantification of cardiolipin molecular species in *Escherichia coli* lipid extracts using liquid chromatography/electrospray ionization mass spectrometry. Rapid Commun Mass Spectrom. 2012;26:2267–74. doi:10.1002/rcm.6350.
42. Granafei S, Losito I, Salivo S, Tranchida PQ, Mondello L, Palmisano F, et al. Occurrence of oleic and 18:1 methyl-branched acyl chains in lipids of Rhodobacter sphaeroides 2.4.1. Anal Chim Acta. 2015;885:191–8. doi:10.1016/j.aca.2015.05.028.
43. Imhoff JF, Bias-lmhoff U. Lipids, quinones and fatty acids of anoxygenic phototrophic bacteria. In: Blankenship RE, Madigan MT, Bauer CE, editors. Anoxygenic photosynthetic bateria. Dordrecht: Kluwer Academic; 1995. p. 179–205.